



# Green synthesis of silver and zinc oxide nanoparticles for novel application to enhance shelf life of fruits

Maria Zafar<sup>1</sup> · Tahir Iqbal<sup>1</sup>

Received: 9 February 2022 / Revised: 15 April 2022 / Accepted: 23 April 2022 / Published online: 5 May 2022  
© The Author(s), under exclusive licence to Springer-Verlag GmbH Germany, part of Springer Nature 2022

## Abstract

Green nanotechnology is fast growing in feasible precision agriculture that assures to refashion food production. This work presents the silver (Ag) and zinc oxide (ZnO) nanoparticles (NPs) synthesized by the green synthesis method. The morphology, composition, structure, size, and purity have been confirmed by and characterized by scanning electron microscopy (SEM), energy-dispersive X-ray (EDX) analysis, X-ray diffraction (XRD) analysis, Fourier transform infrared (FTIR) spectroscopy, and photoluminescence (PL). The optical energy band gap for Ag and ZnO NPs was 2.5 eV and 3.5 eV respectively as investigated by UV–visible spectroscopy. The primary goal of this study is to develop eco-friendly biosynthesized nanoparticles that enhance the shelf time of fruits at room temperature. For this purpose, the different concentrations of Ag and ZnO nanostructures (100 ppm, 500 ppm, and 1000 ppm) have been applied to apples and lemons to study the influence on their shelf life. The PWL% and PO are employed by using a 5-point scale to calculate shelf time correctly. Moreover, periodic measurements have been performed over the coated apple and lemon samples to understand the chemistry and physics behind improvements in shelf life. In contrast to Ag NPs, ZnO NPs present low weight loss at 100 ppm and 1000 ppm. The weight loss percentage of lemon showed direct relation with a concentration of ZnO NPs, whereas inverse for the case of Ag NPs due to strong pathogenic effects of ZnO NPs. These nanoparticles can be easily synthesized by using freely available neem leaves and highly useful for the agricultural industry and food sectors around the globe.

**Keywords** Environmental friendly · Fresh produce · Shelf time enhancement · Ag and ZnO NPs · Physiological weight loss · Physical appearance

## 1 Introduction

Fresh produce is an extensive and essential fountainhead of micro-nutrients and phytochemicals which are required for human well-being. Habitual intake of fresh produce lessens the chance of various chronic diseases [1]. It is known that in developing countries, fruits and vegetables show postharvest losses due to poor technology and mishandlings on different stages. In 2009, according to the Food and Agriculture Organization, 32% of all food produce was unable to use in the world due to poor postharvest treatments [2]. Fruits are also a major source to increase revenue, so

maintenance of good quality and prevention of postharvest losses of fruits are very important. Furthermore, Sandhya et al. also studied that more than 22% fruits were lost due to poor postharvest treatments at different stages [3]. To reduce postharvest losses at various periods in fresh produce [4], nanotechnology has emerged applications that have been utilized in biological sciences, biotechnology, and chemistry [5, 6]. In addition, Ruffo and coworkers have studied that to maintain postharvest technologies, nanotechnology is really supportive in managing postharvest mishandlings, establishing advancements for packaging films, blocking hazardous radiations, and developing nano-biosensors to label fresh commodities [7, 8].

Nanotechnology also introduced nanoparticles that have been utilized as antifungal agents in fresh products [9, 10].

Moreover, the present work also investigated the significance of nanoparticles owing to unique characteristics and their potential applications in food sciences

✉ Maria Zafar  
maria.zafar76@gmail.com

✉ Tahir Iqbal  
tiqbal02@qub.ac.uk

<sup>1</sup> Department of Physics, Faculty of Sciences, University of Gujrat, Gujrat 50700, Pakistan

[11] and agriculture industries [12, 13]. Nanoparticles could be prepared by using various techniques including chemical, physical, and other biological approaches with desiderate conditions. At present, physical and chemical synthesis methods shift towards green synthesis [14] because of their eco-friendly [15], less expensive, and non-toxic nature [16–18]. Due to the unique properties of green synthesis, it exhibits many promising applications such as green electrochemical sensors [19]. Metallic nanoparticles [20] such as Ag NPs are also accustomed to increase shelf life of fresh produce [21]. In the recent few years, Ag and ZnO NPs reported extensively due to their significant antimicrobial attributes [22–25]. Recently, Ag NPs have become the main focus of researchers due to their effective antiseptic properties [26] and serve as efficient antibiotic agents [27]. Owing to unique antimicrobial attributes, ZnO NPs are significantly utilized in many promising applications [28, 29] especially to enhance the shelf time of fruits [30]. Moreover, Rambabu et al. have observed that ZnO NPs are stable antibacterial agent [31] for waste water treatment as compared to organic antimicrobial agents [32–34]. Recently, researchers produce good quality fruits with less postharvest mishandlings by using innovative applications of nano science [35].

In this study, silver nanoparticles (Ag NPs) and zinc oxide nanoparticles (ZnO NPs) were prepared using non-toxic and effective approach using easily available neem leaves. During biosynthesis, green plant leaf extract acts as an oxidizing and a reducing agent. Furthermore, this study evaluates the effect of Ag and ZnO NPs on the shelf time of lemon (*Citrus × limon*), apple (*Malus domestica*), and etc.

## 2 Materials and methods

### 2.1 Precursors

Zinc acetate dihydrate  $Zn [CH_3CO_2]_2 \cdot 2H_2O$ , silver nitrate  $[AgNO_3]$ , and sodium-hydroxide  $[NaOH]$  have been purchased from Sigma-Aldrich, Germany. For both experiments, fresh neem leaves have been taken from the University of Gujrat and deionized water was used as a solvent.

### 2.2 Mechanism of green synthesis of Ag and ZnO NPs

#### 2.2.1 Biosynthesis of silver nanoparticles

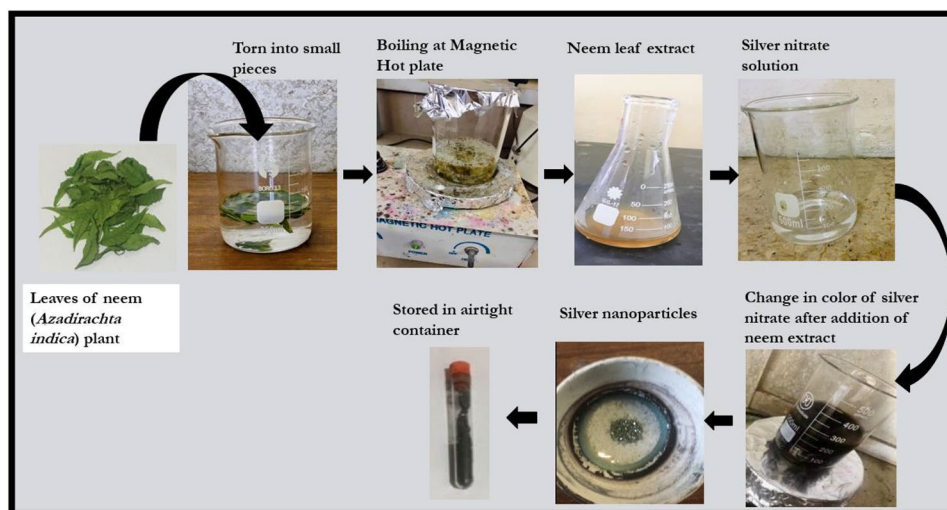
The Ag NPs have been prepared due to the reaction of  $AgNO_3$  and leaf extract of fresh neem (*Azadirachta indica*) leaves. To prepare a homogenous solution of silver nitrate, it is dissolved into the desired amount of distilled water in the beaker of 250 ml. Then, the watery mixture of neem leaves has been added dropwise in the already formulated mixture of  $AgNO_3$  during continuous stirring. Addition of neem leaf extract in silver nitrate solution changes its color from colorless to brown as demonstrated in Fig. 1.

Due to the reduction of Ag salt to Ag NPs, neem leaves exhibit various biomolecules that are responsible for reduction of silver salt to Ag NPs. The Ag NPs present a yellowish brown color because of surface plasmon resonance effect [36].

#### 2.2.2 Biosynthesis of zinc oxide nanoparticles

Biologically synthesized ZnO NPs have been obtained by zinc acetate dihydrate  $Zn (CH_3CO_2)_2 \cdot 2H_2O$  and leaf extract of dry neem leaves. To prepare a homogenous solution of

**Fig. 1** Schematic of green synthesis of silver nanoparticles by using neem leaf extract



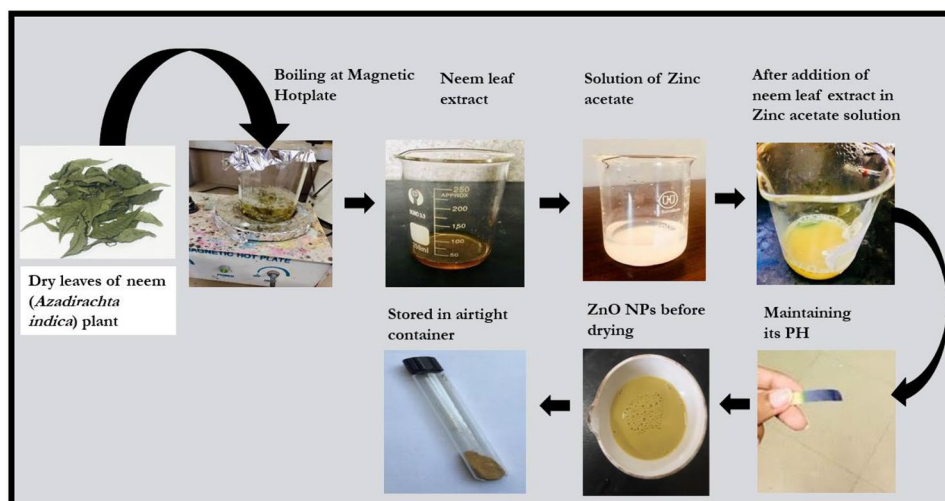
zinc acetate dihydrate, it is dissolved into the desired amount of distilled water in the beaker of 250 ml by using a magnetic stirrer. The aqueous solution of neem leaf extract was prepared by the neem leaves that have been thoroughly washed several times with deionized water and dried at room temperature. A total of 20 g of dried leaf powder has been boiled at 60 °C for 30 min in 100 ml of distilled water. After boiling, the mixture's color converted to pale-yellowish color. Then, the solution has been cooled at room temperature and filtered. Then in the prepared solution of zinc acetate dihydrate, the filtered aqueous solution of *Azadirachta indica* (neem) has been added dropwise during firm stirring. For PH maintenance, aqueous solution of NaOH has been added dropwise during continuous stirring. After addition of neem leaf extract in to zinc acetate dihydrate solution, then color of the solution changed into deep yellow-colored paste due to reduction of zinc ions into ZnO NPs which happened because of excitation of surface plasmon vibrations [37].

Then, the prepared solution has been stirred for 2 h. These deep yellow precipitates have been heated at 400 °C for 3 h in a muffle furnace. Deep yellow-colored powder has been obtained. The obtained product has been grounded and collected in the airtight container for further use as presented in Fig. 2.

### 3 Characterization studies

1. Scanning electron microscopy (SEM) by using SEM-JSM-5910 (JEOL, Japan)
2. Energy-dispersive X-ray (EDX) spectroscopy by using EDX attached with SEM-JSM-5910 (INCA 200/Oxford, UK)
3. X-ray diffraction (XRD) spectroscopy by using JDX-3532 diffractometer (JEOL, Japan)
4. Ultraviolet–visible spectroscopy (UV–visible) by using UV-1800 spectrophotometer (SHIMADZU, India)

**Fig. 2** Schematic of green synthesis of zinc oxide nanoparticles by using neem leaf extract



5. Photoluminescence (PL) spectroscopy by using FP-8200 spectrofluorometer (JESCO, Spain)
6. Fourier transform infrared (FTIR) spectroscopy by using Nicolet iS5 FTIR spectrometer (Thermo Scientific, USA)

## 4 Results and discussions

The Ag and ZnO NPs were synthesized biologically using neem leaf extract. The size and shape of both types of NPs have been studied by scanning electron microscopy. The EDX has been utilized to analyze the chemical composition of the synthesized samples. The XRD gives information about the structure while absorption spectra and band gap have been properties and have been analyzed by UV-vis spectroscopy. The bandgap-related information has been extracted through PL and FTIR analysis. Then, both types of NPs have been applied on apples and lemons to increase their shelf life. Shelf life of fresh produce mainly depends on different factors such as weight loss, firmness, texture, and color of the fruits. This chapter includes detail of all results assessed in this research work.

### 4.1 Morphological evaluation of Ag and ZnO NPs

To analyze the shape and size of biologically prepared silver and zinc oxide NPs, SEM-JSM-5910 (JEOL, Japan) has been used. The Ag NPs were analyzed at different magnification and scale bar lengths during which the accelerating voltage of the beam is 15 kV. Morphology was observed with various magnification powers at different bar lengths including (a) 1000× at 10 μm bar length, (b) 2500× at 10 μm, (c) 10,000× at 1 μm, (d) 5000 at 5 μm, and (e) 30,000× at 0.5 μm. Figure 3 shows the uniform sized agglomerations of spherical Ag NPs. The bar length and magnification power are used to determine the size of nanoparticles. The length

of line bar has been found accurately by dividing the bar length by magnification power and average. To find out the average size of nanoparticles, the number of particles on the line bar has been counted manually and dividing the bar length by the number of particles present on the line bar. In Fig. 3, the SEM images demonstrate the size of the nanoparticles ranging from ~10 to 50 nm. Similarly, the morphology of biologically synthesized ZnO NPs was also analyzed by scanning electron microscope at 15 keV accelerating voltage. Patra et al. have also investigated that the pH of solution can significantly affect the morphology of silver nanoparticles [38]. Thus, in this case of Ag and ZnO NPs, pH of the solution is 7 and 13 that control their morphologies respectively. The SEM images have been taken at various bar lengths with different magnification powers: (a) 2500 $\times$  at 10  $\mu$ m bar length, (b) 10,000 $\times$  at 1  $\mu$ m, (c) 15,000 $\times$  at 1  $\mu$ m, (d) 30,000 $\times$  at 0.5  $\mu$ m, and (e) 60,000 $\times$  at 0.25  $\mu$ m as demonstrated in Fig. 3.

The SEM images in Fig. 3 show that Ag and ZnO NPs have spherical, cubical, bean-like, and irregular shapes due to heating effects [39] and the size of the ZnO NPs ranges from ~5 to 80 nm. Moreover, Rai et al. have also reported

that the nature of NPs is significantly affected by the temperature during the synthesis of NPs [40].

## 4.2 EDX analysis of Ag and ZnO NPs

The energy-dispersive X-ray (EDX) analysis is an X-ray technique utilized to recognize the elemental configuration of materials. The quantitative investigation of samples was accomplished using the EDX method at ambient temperature to analyze the stoichiometry of metallic and metallic oxide nanoparticles. The EDX analysis has been observed in the energy region of 20 keV by using EDX attached with SEM-JSM-5910 (INCA 200/Oxford, UK). Figure 4a presents the existence of Ag peaks that confirm the synthesis of Ag NPs with an average composition of 88.39% Ag and 11.6% due to silver reaction with air. There is no extra peak that confirms the purity of both samples.

Similarly, Fig. 4b confirms the presence of ZnO NPs in the sample as strong peaks are present. The atomic weight of ZnO is 69.32% and O is 30.69% present in the sample. Figure 4c gives comparison of elemental analysis of Ag and ZnO NPs.

**Fig. 3** Morphological evaluation of biosynthesized **a, b** silver nanoparticles and **c, d** zinc oxide nanoparticles

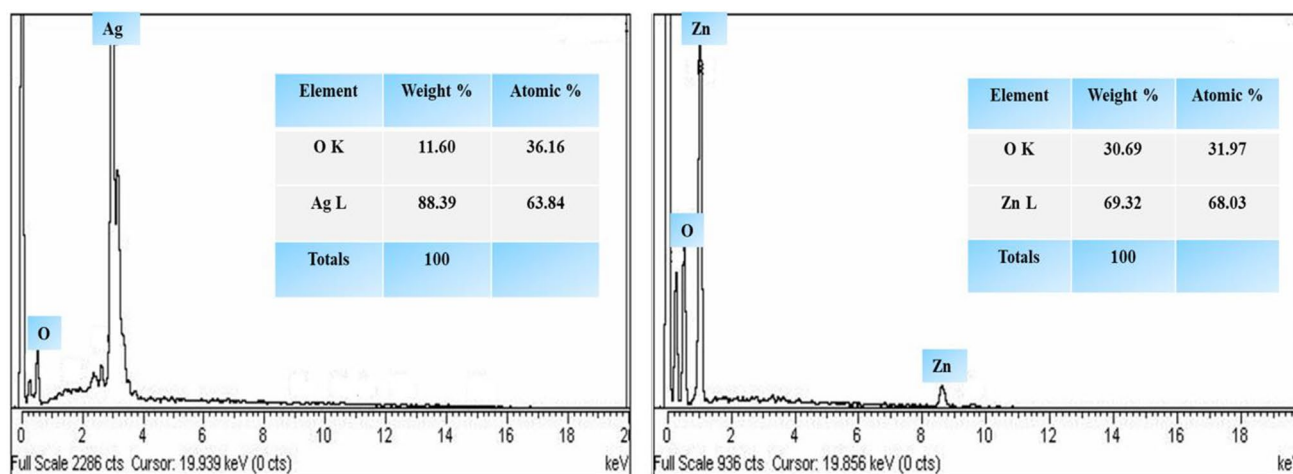
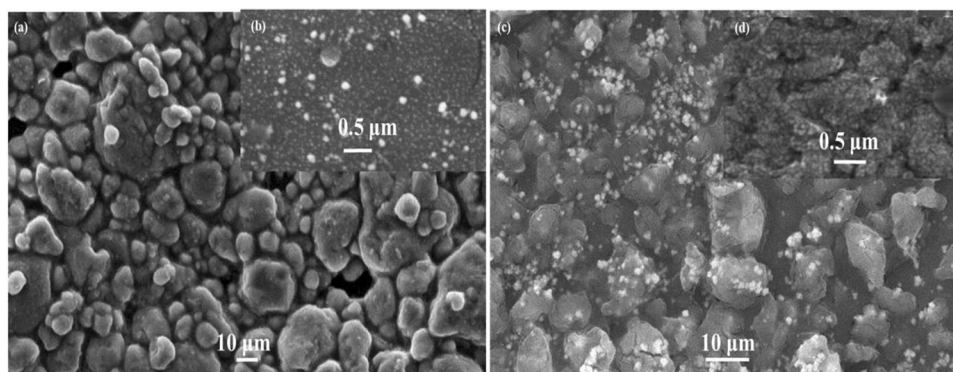


**Fig. 4** EDX interpretation of biosynthesized **a** Ag NPs and **b** ZnO NPs

### 4.3 Structural analysis of green synthesized Ag NPs and ZnO NPs

X-ray diffraction analysis is the most useful method by which X-rays of familiar wavelength are proceed through a sample to investigate the crystalline structures. The phase identification of the silver nanoparticles was also carried out by X-ray diffraction method. The sample was grounded using a mortar and pestle into powder. X-ray powder diffraction measurement was carried out by using JDX-3532 diffractometer (JEOL, Japan) with long fine focus copper tube operated at 40 kV and 30 mA in Bragg–Brentano geometry. The X-ray detector moves throughout the sample at an angle  $2\theta$  to calculate the intensity and position of the diffracted peaks. The high intensity peak is known as the highest peak and the other peaks have been observed as compared to the highest peak. The powder XRD data were obtained in the  $2\theta$  range from 5 to  $80^\circ$  in step-scan mode with  $2\theta$  step of  $0.02^\circ$ . The X-ray diffractometer was calibrated by means of external silicon standard, SRM 640a. The diffraction pattern indicated that the sample is the silver nanoparticles. The conversion of silver nitrate to silver nanoparticles was greater than 90% which is due to potential reduction of Ag NPs during preparation at ordinary pressure which is in accordance with the study of Patra and coworkers [38]. Pandey et al. have also investigated that the structural attributes of biosynthesized NPs are significantly affected by the pressure applied to the reaction medium [41]. It is also found that these Ag NPs present smaller peaks due to neem extract impurities. The XRD pattern of green synthesized Ag NPs is clearly shown in Fig. 5. This type of spectra shows labeled peaks. These Ag peaks show diffraction spectra from 20 to  $100^\circ$  at  $2\theta$  angle with  $30.42^\circ$ ,  $44.60^\circ$ ,  $64.71^\circ$ ,  $77.61^\circ$ , and  $81.84^\circ$  values respectively on (111), (222), (311), and (200) according to the JCPDS card number 87–0719.

This analysis demonstrates the nanocrystals of Ag NPs with size 31.9 nm which has been calculated using Debye–Scherrer formula. Pandey and coworkers have investigated that the structural attributes of biosynthesized NPs are significantly affected by the pressure applied to the reaction

medium [41]. In addition, Patra et al. have studied that during green synthesis of Ag NPs, the rate of reduction increases at ordinary pressure [38]. Moreover, the Ag peaks are shown at  $2\theta$  values of  $31.947^\circ$ ,  $33.910^\circ$ ,  $36.431^\circ$ ,  $47.717^\circ$ ,  $56.765^\circ$ ,  $63.029^\circ$ ,  $68.086^\circ$ ,  $69.220^\circ$ , and  $77.679^\circ$  at (100), (002), (101), (102), (101), (103), (112), (201), and (202) points. This XRD pattern is in good agreement with JCPDS# 79–0205. The particle size of zinc oxide nanoparticles was determined by Debye–Scherrer formula which is 49 nm.

### 4.4 UV–visible investigation of Ag and ZnO NPs

The absorption properties of the synthesized samples have been calculated and analyzed by UV–visible spectrum which is achieved by using a UV-1800 spectrophotometer (SHIMADZU, India) in the wavelength of 200–800 nm. The bandgap of both samples has been evaluated by deducing Tauc plot from UV–visible spectrum which gives the relation between energy of photons ( $h\nu$ ) and optical absorption coefficient ( $\alpha$ ) presented in Eq. 1:

$$ah\nu = A(h\nu - E_g)^n \quad (1)$$

where  $A$  is expressed as the effective mass of the materials,  $E_g$  is also called the band gap energy, and  $n$  is presented as the type of transition of samples. Direct transitions exhibit  $n = 1/2$ , indirect have  $n = 2$ , and forbidden transitions present  $n = 3/2$ . The wavelength and absorption spectra are taken on horizontal and vertical axis as shown in Fig. 6. It also presents that the graph between wavelength and absorption spectrum has been obtained because of noteworthy phenomenon of surface plasmon resonance (SPR), which is a significant absorption of light waves manifested by Ag NPs in the visible region [42]. The SPR phenomenon occurs when NPs are exposed by the detectable light, due to the united vibrations of the negatively charged free electrons. The SPR peak also confirmed the presence of neem leaf extract due to reduction of silver ions to silver NPs from  $\text{AgNO}_3$  solution. The bandgap of these biologically synthesized Ag NPs is also shown in Fig. 6a by using Tauc plot that gives the

**Fig. 5** The structural analysis of biosynthesized **a** Ag NPs and **b** ZnO NPs

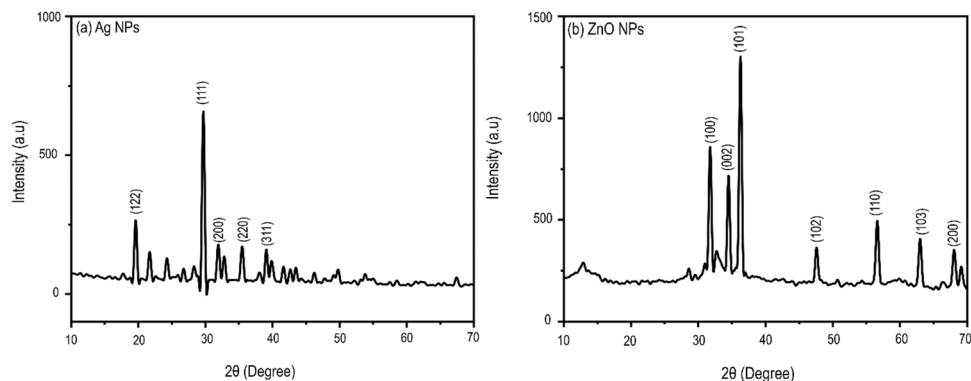
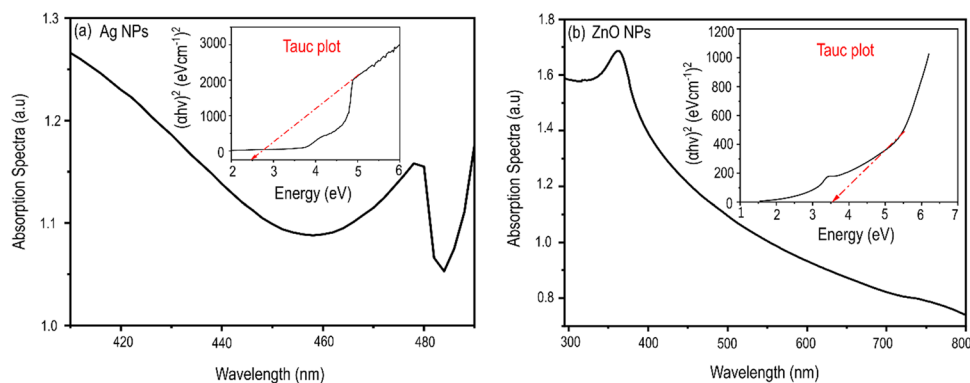


**Fig. 6** The absorption spectrum and Tauc plot of green synthesized **a** Ag NPs and **b** ZnO NPs



information about photon energy ( $h\nu$ ) and optical absorption coefficient ( $\alpha$ ), constant  $A$ , and  $E_g$  as illustrated above. The absorption spectrum of given samples is size dependent due to SPR band dependence upon size and refractive index of the sample [42].

Amendola et al. have investigated that the absorption spectrum of a given sample of Ag NPs is size dependent due to SPR band dependence upon size and refractive index of the sample [42]. The bandgap of green synthesis Ag NPs is 2.5 eV which is the same as obtained from Tauc's formula. This graphical representation of green synthesized Ag NPs also shows that sample 1 (1.5 ml extract concentration) shows 1.4 absorption at 320 nm wavelength which decreases gradually as wavelength increases but at 400 nm, absorbance has been recorded at 1.25 which gradually decreases to 1.15 at 800 nm wavelength. After this, at 470 nm wavelength, it gradually increases up to 1.5 at 550 nm wavelength [43]. The above analysis shows that green synthesized Ag NPs exhibit high absorption intensity and sharp SPR peaks due to presence of phytochemicals of neem leaf extract which acts as capping and stabilizing agent [44]. He et al. have reported that longer irradiation time also causes higher plasmon absorption and shifts towards longer wavelengths due to larger particle size [45]. Noorjahan et al. have found that the ZnO NPs exhibit free electrons, which are responsible for the surface plasmon resonance absorption band evolution that is due to the collective electronic vibrations of metallic NPs in resonance with electromagnetic waves [46]. The UV–visible spectrum and band gap of green synthesized ZnO NPs are also calculated by Tauc plot that is 3.5 eV as illustrated in Fig. 6b. In this case (1.5 ml neem leaf extract), at 350 nm wavelength, absorption has been observed as 1.7 absorbance that decreases step by step and at 800 nm, it has been 0.9 [43]. To explain this type of absorption spectra, Ahmed et al. have reported that high absorption intensity of SPR peaks is due to greater concentration of neem leaf extract [44]. In the above analysis, the SPR peak of green synthesized ZnO NPs confirmed the higher concentration of neem leaf extract because it exhibits significant concentration of biomolecules such as terpenoids and flavanones that play significance in

the reduction of metallic NPs. Fakhari and coworkers have reported that increase in band gap causes decrease in the particle size and their absorption wavelength [47]. Moreover, the spectroscopic analysis of both types of NPs has been analyzed at 25 °C and the absorption spectra of both Ag and ZnO NPs are owing to confinement of electron–hole pairs in smaller regions that gives more absorption of light and it was observed that Ag and ZnO NPs exhibit unbending nature of spectrum that is why both types of NPs are known as direct transition type materials.

#### 4.5 Photoluminescence analysis of green synthesized Ag and ZnO NPs

The PL spectra of biosynthesized Ag NPs have been examined by FP-8200 spectrofluorometer (JESCO, Spain) at room temperature as presented in Fig. 7. These Ag NPs show the excitation wavelength at 365 nm that demonstrates broad emission peak at 415 nm and PL intensity of fluorescence emission peak increases step by step up to 415 nm; then, quite interestingly it gradually decreases up to 619 nm [48]. In recent few years, Anandalaksh et al. have reported the broader emission spectra at 478 nm [49].

The PL spectra of all biosynthesized samples of Ag NPs have been measured by using FP-8200 spectrofluorometer that show the excitation wavelength at 365 nm. At this excitation wavelength, it shows PL fluorescence emission peak intensity at 412 nm that is demonstrated in Fig. 7a. Jiang et al. have found the fluorescence peak of silver NPs at 465 nm in liquid phase [48]. Anandalaksh et al. have reported the broader emission spectra at 478 nm [49]. Figure 7 shows blue shifted emission peak as compared with previously reported PL spectra at 465 nm and 478 nm. Similarly the PL analysis of ZnO nanoparticles gives significant information about its purity and quality. Generally, it contains two emission peaks including UV peak closer to the band edge emission and visible peak due to deep level emission (DLE) bands [50, 51]. Due to optical intrinsic imperfections, this affects the optical characteristics of ZnO and other types of defects are produced during preparation, growth, and

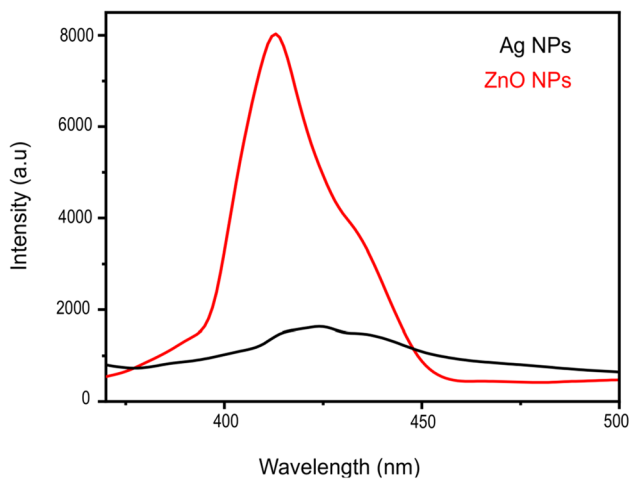


**Fig. 7** The PL spectra of green synthesized silver nanoparticles (Ag NPs) and zinc oxide nanoparticles (ZnO NPs)

annealing. The PL spectra of green synthesized ZnO NPs using neem leaf extract are measured by FP-8200 spectrofluorometer as demonstrated in Fig. 7b. These biosynthesized ZnO NPs present the sharp emission peak at 428 nm. This type of UV emission is due to near band edge transitions, exciton-exciton collisions, and free exciton recombination. In the green synthesis method, due to chemical interaction among biomolecules that are present in neem leaf extract, the ZnO NPs create imperfections that significantly affect their emission properties. This type of UV emission is due to near band edge transitions, exciton-exciton collisions, and free exciton recombination. The biosynthesized ZnO NPs manifest passive defects that have been created

due to chemical interaction between biomolecules which are present in neem leaf extract that significantly influence on the emission properties [52].

#### 4.6 FTIR analysis of green synthesized Ag NPs and ZnO NPs

The FTIR analysis of green synthesized Ag NPs has been carried to examine the functional groups existing in neem leaf extract that acts as reducing and capping agents during synthesis process of Ag NPs [53] by using Nicolet iS5 FTIR spectrometer (Thermo Scientific, USA). The observed spectra of Ag NPs have been compared with previously reported literature to determine the functional groups present in it. In Fig. 8a, sample 1 of Ag NPs presents absorption peaks at 3355.62, 2349.07, 1771.88, 1751.93, 1619.80, 1267.68, 799.17, and 731.04  $\text{cm}^{-1}$ . In IR spectra, the absorption bands at 3379.51  $\text{cm}^{-1}$  are related to N–H stretching vibrations that indicate the presence of amine functional groups. At 2347.526  $\text{cm}^{-1}$ , absorption peaks show C–H stretching vibrations due to aromatic compounds observed. The absorption band at 1771.88  $\text{cm}^{-1}$ , 1751.93  $\text{cm}^{-1}$ , and 1619.80  $\text{cm}^{-1}$  corresponded to the C=O and C=C stretching vibrations and exhibits anhydride and alkene functional groups respectively. The absorption peaks at 1267  $\text{cm}^{-1}$  are because of carbon–nitrogen-based functional groups [54] and the absorption bands at 799.17 and 731.04  $\text{cm}^{-1}$  have been analyzed due to presence of aromatic compounds in it.

Similarly, in case of biosynthesized ZnO NPs, the FTIR spectra also present two regions including the functional group region that examined functional groups that exist in the neem leaf that has been utilized in biosynthesis of ZnO

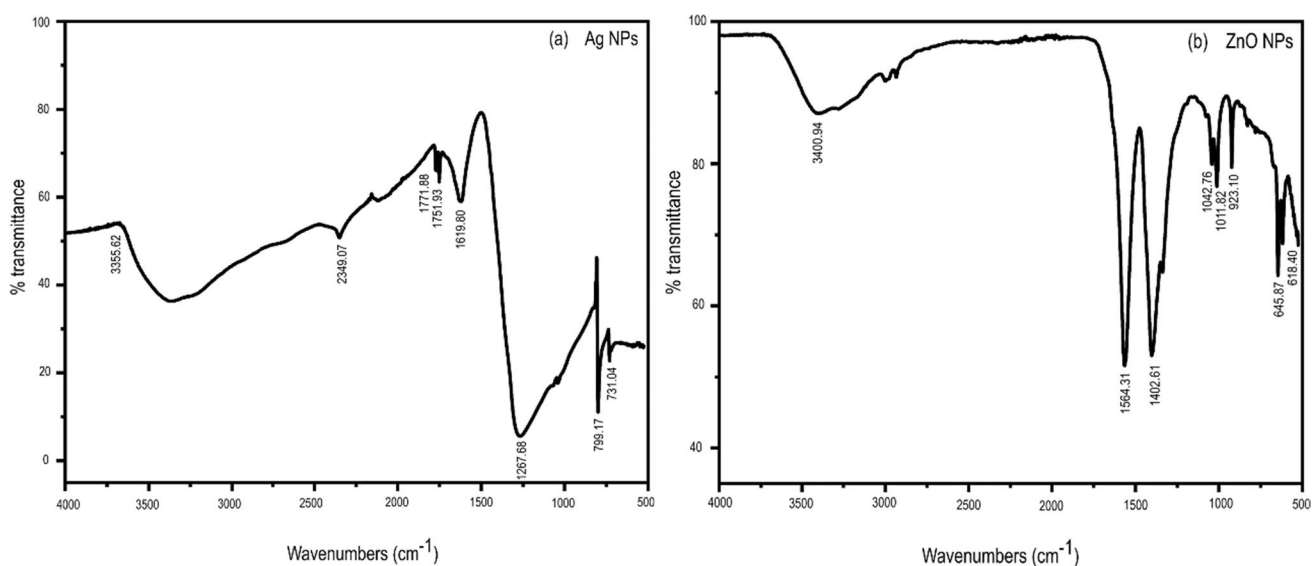


**Fig. 8** The FTIR spectra of biosynthesized **a** Ag NPs and **b** ZnO NPs

**Table 1** Comparison table to summarize literature studies of Ag and ZnO nanoparticles utilized for shelf time enhancement

Type of nanoparticles	Synthesis method	Increase in shelf time	Effect on shelf life of fruits	References
Silver NPs	Green synthesis	15 days	Cherry tomatoes	[66]
Silver NPs	Green synthesis	-	Pear	[67]
Agar-silver NPs	Green synthesis	-	Lime and apple	[68]
Zinc oxide NPs	LPDE NCs films	16 days	Fresh strawberry	[69]
Silver montmorillonite NPs	Edible coating	5 days	Fresh fruit salad	[70]
SLN NPs and xanthan gum	Active packaging	-	Guava	[71]

nanoparticles and the finger-print region. These functional groups are responsible for stability due to its stabilizing and capping nature. Figure 8b also shows that ZnO NPs demonstrate the absorption bands at 3408.50, 1634.40, 1545.90, 1405.87, 1018.46, 926.50, 795.84, and 638.51  $\text{cm}^{-1}$ . The absorption band at 3408.50  $\text{cm}^{-1}$  demonstrated that this belongs to the O–H functional group. At 1634.40  $\text{cm}^{-1}$  of absorbance, peaks indicated the C=O stretching vibrations due to presence of amines. The FTIR spectra at 1545.90  $\text{cm}^{-1}$  indicate the nitrogen–oxygen stretching vibrations. At 1405.87  $\text{cm}^{-1}$ , it indicates the presence of aromatic compounds. At 1018.46  $\text{cm}^{-1}$ , it shows the presence of alkyl groups due to C–O stretching vibrations. When the FTIR analysis presents the absorption band at 926.50, 795.84, and 638.51  $\text{cm}^{-1}$  which indicates its correspondence with aromatic compounds that is illustrated in Fig. 8b, therefore this confirms the presence of phytochemicals in it that are responsible for the green synthesis process of ZnO NPs.

#### 4.7 Mechanism of shelf time enhancement

The biosynthesized nanoparticle-based shelf time enhancement process directly linked with antimicrobial properties of nanoparticle [55]. Those green synthesized Ag and ZnO nanoparticles exhibit a high surface to volume ratio as

compared to their bulk counterparts. Due to wide surface area, the interactions with the bacterial surfaces are facilitated, and antibacterial properties become enhanced [56]. Ahmed et al. have studied that the antimicrobial properties of green synthesized nanoparticles are dependent upon the size and living circumstances and capping agent. The positive charge on the Ag and ZnO ions is crucial for antimicrobial activities. In ionic form, Ag and ZnO NPs have the ability to form complexes and can act as an excellent antimicrobial agent [57]. Several studies have reported that there is a great electrostatic attraction between  $\text{Ag}^+$  and  $\text{Zn}^{2+}$ -based Ag and ZnO NPs and bacterial cells [58] and has been considered significant bactericidal agent [59, 60]. These NPs can assemble themselves inside the cell membrane and can eventually cause damage to cell wall or cell membranes. Other mechanisms include interaction of nanoparticles with biological macromolecules such as enzymes and DNA through an electron-release mechanism [61] or free radical production [62]. Nanoparticles have been considered a powerful antimicrobial agent against bacterial and fungal species. Several researchers have investigated that both Ag and ZnO NPs can change the geometry of proteins by interfering with disulfide bonds and block the functional effects of the bacteria, viruses, and fungi [63, 64]. By using cost and eco-friendly route-based nanoparticles, it is very easy to achieve improvement in shelf time of fresh produce [65].

The abovementioned table (Table 1) demonstrates the literature related to green synthesized silver and zinc oxide-based nanoparticles that has been used to improve the shelf life of fresh commodities.

**Table 2** PWL% analysis of stored apples

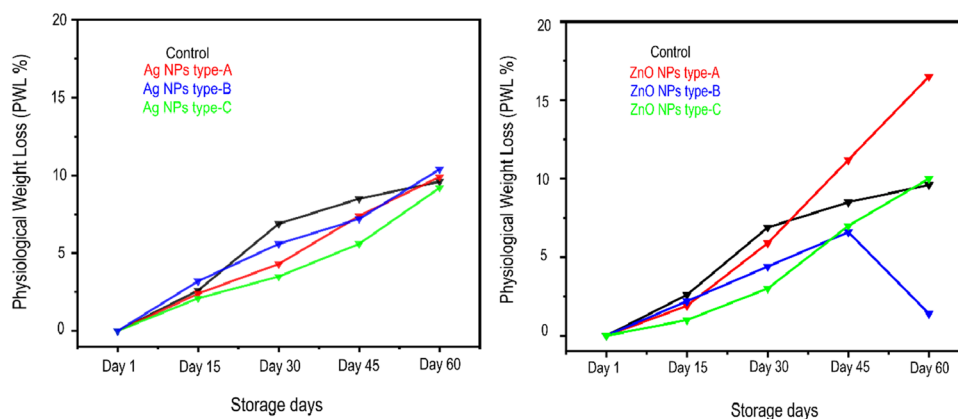
Apple samples	Day 1	Day 15	Day 30	Day 45	Day 60
Controlled (0 ppm)	0	2.6	6.9	8.5	9.6
Ag NPs type A (100 ppm)	0	2.4	4.3	7.4	9.9
Ag NPs type B (500 ppm)	0	2.1	3.5	5.6	9.2
Ag NPs type C (1000 ppm)	0	3.2	5.6	7.2	10.4
ZnO NPs type A (100 ppm)	0	1.9	5.9	11.2	16.5
ZnO NPs type B (500 ppm)	0	2.2	4.4	6.6	1.4
ZnO NPs type C (1000 ppm)	0	1	3	7	10

##### 4.7.1 Preparation of Ag NPs and ZnO NP solutions for coating

A total of 100 ppm Ag NPs and ZnO NP solution was achieved by using 0.1 g of Ag NPs and ZnO NPs into 1000 ml of deionized water. Similarly, 500 ppm and 1000 ppm Ag NPs and ZnO NP solution have been obtained from 0.5 g and 1 g of respective nanoparticles. All solutions were stirred at 25 °C for coating purposes. Finally, it



**Fig. 9** a Effect of type A, type B, and type C of Ag and b ZnO NPs on weight loss percentage of stored apples



is observed that a total of six solutions were prepared, three based on Ag NPs and the other three include ZnO NPs.

for storage purposes. Apart from this, a few apple and lemon samples have been utilized as controlled samples.

**4.7.2 Coating of prepared nanoparticle-based solutions on apples and lemons**

**4.7.3 Effect of Ag and ZnO NPs on shelf time of fruits**

The shelf time of fresh apples and lemon has been calculated by two parameters which have been described below.

**Table 3** PWL% analysis of stored lemons

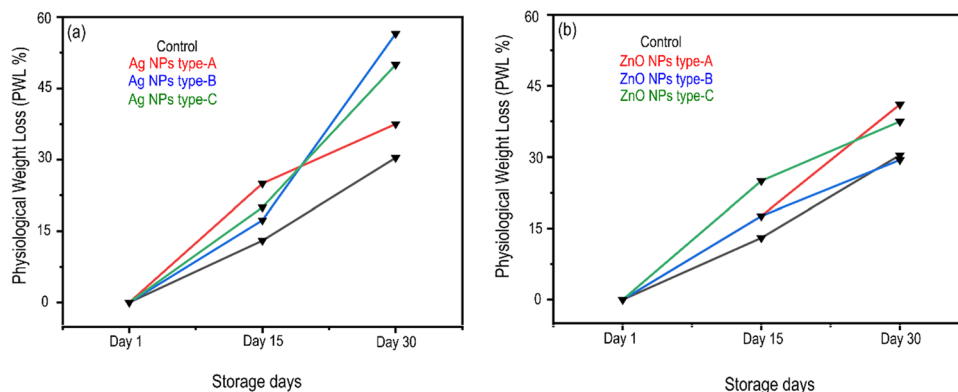
Lemon samples	Day 1	Day 15	Day 30
Controlled (0 ppm)	0	13	30.4
Ag NPs type A (100 ppm)	0	25	37.5
Ag NPs type B (500 ppm)	0	17.3	56.5
Ag NPs type C (1000 ppm)	0	20	50
ZnO NPs type A (100 ppm)	0	17.6	41.1
ZnO NPs type B (500 ppm)	0	17.6	29.4
ZnO NPs type C (1000 ppm)	0	25	37.5

**A) Physiological weight loss (PWL%) analysis**

After preparation of the abovementioned nanoparticle-based solutions, the apple samples were dipped for 15 min separately for every solution by using 500-ml glass containers. After dipping, the coated samples were kept in petri dishes

Mostly, it is seen that weight loss is directly affected by storage time. To measure the physiological weight loss, there are three categories of fresh apples and lemons including controlled, Ag nanoparticles type A, type B, and type C, and ZnO nanoparticles type A, type B, and type C which are under observation. The digital weight balance has been used to calculate accurate weight of apple and lemon samples. The first group was kept uncoated so these were known as controlled samples. The controlled apples are just ordinary tomatoes which are stored for analysis and comparison. The second class is the apples in which Ag nanoparticles type A (100 ppm solution), type B (500 ppm solution), and type C (1000 ppm solution) have been coated over them. The third kind is in which ZnO nanoparticles type A (100 ppm solution), type B (500 ppm solution), and type C (1000 ppm

**Fig. 10** a Effect of type A, type B, and type C of Ag and b ZnO NPs on weight loss percentage of stored lemon samples



solution) have been coated on fresh apples. After every 15 days, the effect of three different concentrations of Ag and ZnO NPs on weight loss of these three categories is presented in Table 2.

The above tabular data of weight loss of fresh apples has been measured through weight loss formula reported by Haile and coworkers [72] which is shown in Eq. 2.

$$\text{Physiological weight loss(\%)} = \frac{\text{Initial weight} - \text{current weight}}{\text{initial weight}} \times 100 \quad (2)$$

Then, weight loss percentage was examined for all samples of fresh apples and lemons by using weight loss formula. The depictive illustration of storage days and PWL% of stored apples is shown as Fig. 9.

The abovementioned figure (Fig. 9a) demonstrates all concentrations of Ag NPs, and among other concentrations, Ag NP type C causes low weight loss percentage of stored

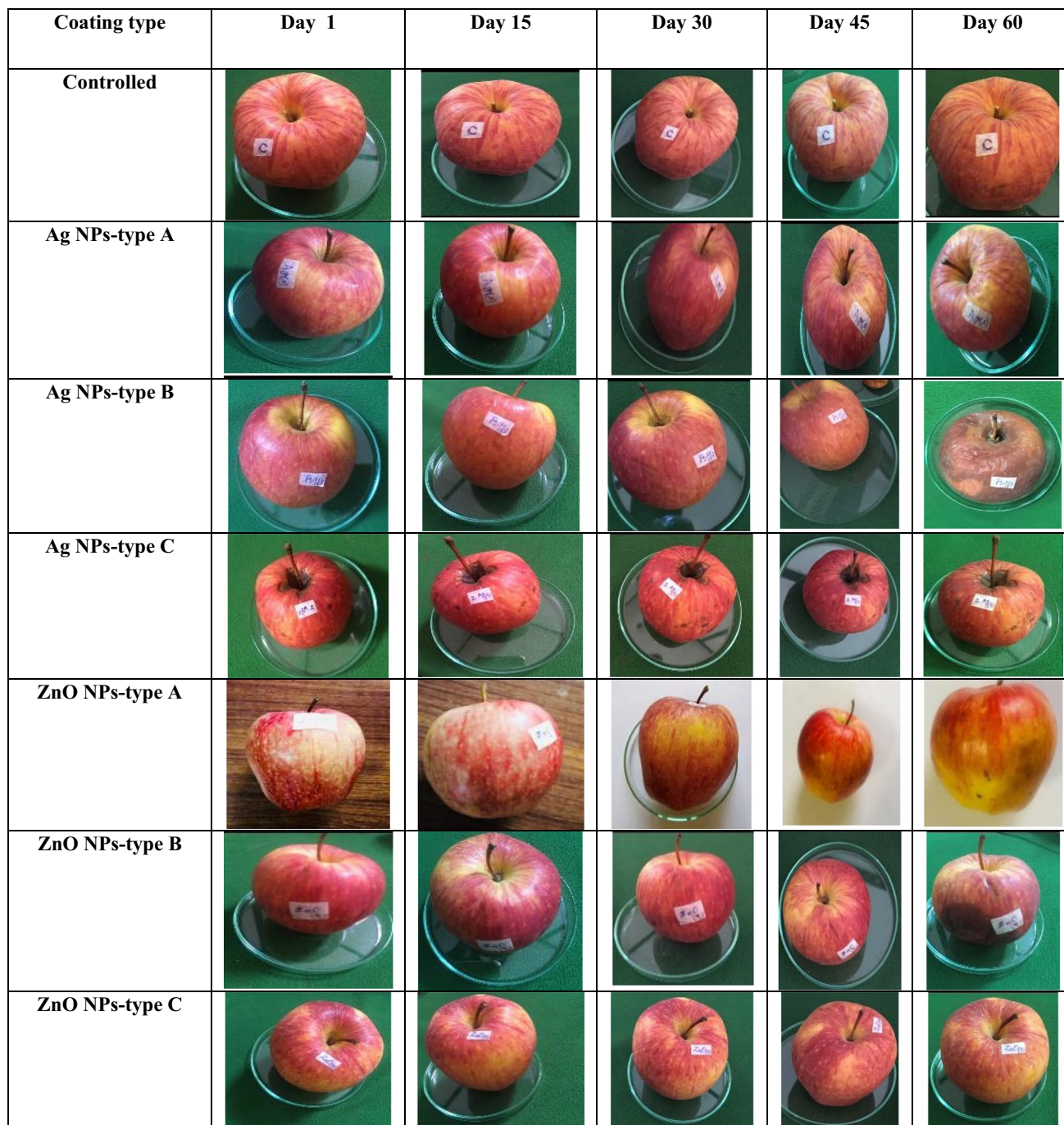


**Fig. 11** Effect of type A, type B, and type C of Ag and ZnO NPs on physical appearance of stored apples and lemons at room temperature

**Table 4** Overall level of appropriateness for stored apples

Overall level of appropriateness					
Unusable = 1, usable = 2, fair = 3, good = 4, excellent = 5					
Apple samples	Day 1	Day 15	Day 30	Day 45	Day 60
Controlled (100 ppm)	5	4	4	1	1
Ag NPs type A (100 ppm)	5	4	3	1	1
Ag NPs type B (500 ppm)	5	4	3	1	1
8ikm Ag NPs type C (1000 ppm)	5	4	1	1	1
ZnO NPs type A (100 ppm)	5	4	3	1	1
ZnO NPs type B (500 ppm)	5	4	4	1	1
ZnO NPs type C (1000 ppm)	5	4	4	2	1

apples. Similarly, the effect of three different types of concentrations of ZnO NPs on weight loss percentage of stored apples is shown in Fig. 9b. In contrast to other concentrations of ZnO NPs, ZnO NP type C causes a low weight loss percentage of stored apples. Similarly, the effect of 100 ppm concentration of Ag and ZnO NPs on weight loss percentage of stored apples is clearly shown in Fig. 9c. The type A concentrations of both Ag and ZnO NPs significantly affect weight loss percentage of stored apples, but as compared to ZnO NPs, Ag NPs showed low weight loss percentage of stored apples. The effect of both types of NPs is compared with controlled samples of fresh apples. Controlled samples show comparable weight loss percentage to both type of NPs at the start but gradually it show very low weight loss percentage in contrast with effects of weight loss on both types of nanoparticles. Similarly, the influence of 500 ppm concentrations of Ag and ZnO nanoparticles on weight loss percentage of stored apples is presented in Figure 9d. In contrast to type B concentration of Ag NPs, ZnO NPs showed low weight loss percentage of stored apples. Similarly, the effect of 1000 ppm concentration of Ag and ZnO NPs on weight loss percentage of stored apples is shown in Figure 9e. The type C concentrations of both Ag and ZnO NPs significantly affect weight loss percentage of stored apples, but as compared to Ag NPs, ZnO NPs showed low weight loss percentage of stored apples. Table 3 presents the physiological weight loss of fresh lemons, when three different types of concentrations of Ag and ZnO have been coated. After every 15 days, the effect of three different concentrations of both types of NPs on weight loss of fresh lemons is seen.

Similarly, the effect of three different types of concentrations of Ag and ZnO NPs on weight loss percentage of stored lemons is shown in Fig. 10.

In this case, three different concentrations of Ag NPs show the same effect at the start but after 15 days, 100 ppm Ag NPs causes a low weight loss percentage of stored lemon samples as compared to other samples that is clearly shown in Fig. 10a. Similarly, the effect of three different types of concentrations of ZnO NPs on weight loss percentage of stored lemon samples is shown in Fig. 10b. Among

other concentrations of ZnO NPs, 500 ppm ZnO NPs causes low weight loss percentage of stored lemon samples. Similarly, the effect of 100 ppm concentration of Ag and ZnO NPs on weight loss percentage of stored lemon samples is demonstrated in Fig. 10c. Both Ag and ZnO NPs of type A significantly affect weight loss percentage of stored lemon samples, but as compared to ZnO NPs, Ag NPs showed low weight loss percentage of stored samples. When coated samples are compared with uncoated samples, then uncoated samples show low weight loss percentage. Similarly, the effect of 500 ppm concentration of Ag and ZnO NPs on weight loss percentage of stored lemon samples is shown in Fig. 10d. In contrast to the weight loss due to type B of both types of NPs, the comparison of the effect of both types of NPs exhibits that the Ag NPs showed low weight loss percentage of stored lemon samples but controlled samples show low weight loss percentage at the start which gradually equals to the Ag and ZnO NP-coated samples. Similarly, the effect of 1000 ppm concentration of Ag and ZnO NPs on weight loss percentage of stored lemon samples is shown in Fig. 10(e). Similarly, the type C of Ag and ZnO NPs significantly affects weight loss percentage of stored apples, but as compared to ZnO NPs, Ag NPs showed low weight loss percentage of stored lemon samples. The present work concluded that when both types of fruits are treated at various concentration of Ag NPs and

**Table 5** Overall level of appropriateness for stored lemons

Overall level of appropriateness			
Unusable = 1, usable = 2, fair = 3, good = 4, excellent = 5			
Lemon samples	Day 1	Day 15	Day 30
Controlled (0 ppm)	5	1	1
Ag NPs type A (100 ppm)	5	2	1
Ag NPs type B (500 ppm)	5	2	1
Ag NPs type C (1000 ppm)	5	2	1
ZnO NPs type A (100 ppm)	5	2	1
ZnO NPs type B (500 ppm)	5	3	1
ZnO NPs type C (1000 ppm)	5	3	1

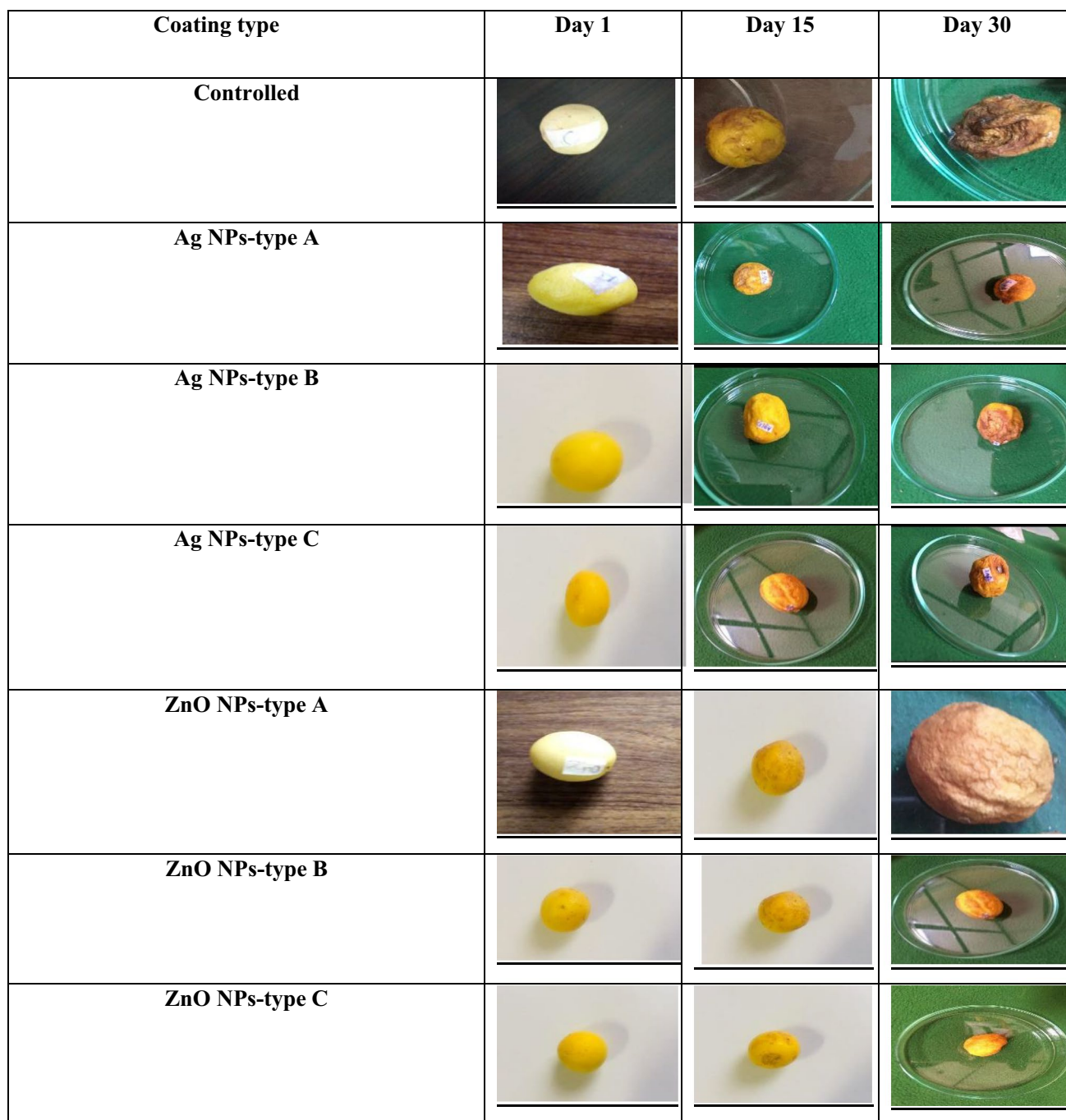


**Fig. 12** Effect of type A, type B, and type C of Ag and ZnO NPs on physical appearance of stored lemons at room temperature

ZnO nanoparticles, the effect of storage time on weight loss percentage is different for different fruit samples. In case of citrus fruits, Abdelmalek et al. have studied that Ag NPs present a significant antifungal efficacy against fungal species including *Alternaria alternata*, *P. digitatum*, and *Alternaria citri*. As already mentioned that silver nanoparticles have potentially damaged the DNA and proteins and consequently cause cell death, so it is concluded that due to

the promising antifungal and antibacterial properties of Ag NPs, the shelf time of citrus fruits can be enhanced [73].

B) Physical appearance and overall appropriateness (PO) analysis

The physical appearance and overall appropriateness have significant effects on consumers.

To measure the PO of fresh apples and lemons, there are three categories of fresh apples and lemons including controlled, Ag nanoparticles type A, type B, and type C, and ZnO nanoparticles type A, type B, and type C which are under observation on planned schedules (Fig. 11). After every 15 days, along with the weight loss, physical appearance such as color, softness, and firmness has been recorded that is shown in Table 4. The abovementioned photographs of fresh apples clearly show their overall physical appearance and acceptability. The sample of three categories including controlled (0 ppm NPs), Ag nanoparticles type A, type B, and type C, and ZnO nanoparticles type A, type B, and type C is under observation. After every 15 days, significant changes have been shown by fresh apple samples. After 45 days, these fresh apples are unusable and the overall acceptability of these fresh apples is described in Table 4.

Similarly, to check the physical appearance and overall acceptance, they are following classifications of lemons including controlled, Ag nanoparticles type A, type B, and type C, and ZnO nanoparticles type A, type B, and type C which are stored for 30 days. The abovementioned photographs of fresh apples clearly show their overall physical appearance and acceptability. The sample of three categories including controlled (0 ppm NPs), Ag nanoparticles type A, type B, and type C, and ZnO nanoparticles type A, type B, and type C is under observation. After every 15 days, significant changes have been shown by fresh apple samples. The abovementioned photographs of fresh apples clearly show their overall physical appearance and acceptability. The sample of three categories including controlled (0 ppm NPs), Ag nanoparticles type A, type B, and type C, and ZnO nanoparticles type A, type B, and type C is under observation. After every 15 days, significant changes have been shown by fresh lemon samples. These samples were observed on planned schedules. After every 15 days, along with the weight loss, physical appearance such as color, softness, and firmness has been recorded that is demonstrated as Table 5. Recent studies reveal that ZnO NPs have excellent antifungal properties especially against *Penicillium expansum*, which is used to control the postharvest mishandlings in lemons, at higher concentrations of ZnO NPs and greatly enhanced the shelf life of fresh lemons. Results also present that ZnO NPs also prevent the growth of conidiophores and conidia [74].

The abovementioned photographs (Fig. 12) of fresh stored lemons significantly show that the color, firmness, and softness can be easily determined by using a 5-point scale which has been discussed already.

It is observed that the PO of lemons was due to mold extension, smoothness, dryness, and glossiness. From the data shown, it is clearly analyzed that the acceptability levels can be examined easily by using the 5-point scale.

## 5 Conclusion

In the present work, silver and zinc oxide nanoparticles have been successfully prepared by green's route in which neem extract has been confirmed by various characterization techniques such as UV–vis, PL, XRD, and Fourier transform infrared spectroscopy. In addition, three different concentrations of both types of NPs have been utilized for coating of both fruits for the shelf time enhancement which was calculated by two factors including PWL % and PO. Consequently, it is investigated that as compared to Ag NPs, the ZnO NPs have been found to better preserve the postharvest quality of apples and lemons. Furthermore, this research work clearly showed that the uncoated samples showed the fastest degradation rate and the coating formulations act positively as a conservative agent by delaying the mass loss for both apples and lemons. Apart from this, it is also concluded that ZnO NPs type C behaves better for apples. In case of lemons, ZnO NPs type B and type C show low weight loss percentage as compared to uncoated and Ag NP-coated fruits. This study is only valid for apples and lemons. On contrary, these findings stimulate more research on the use of Ag and ZnO NPs as food preservatives, with particular scrutiny accustomed to significant safety concerns.

**Supplementary Information** The online version contains supplementary material available at <https://doi.org/10.1007/s13399-022-02730-8>.

**Author contribution** Maria Zafar: writing—original draft, data curation, validation, project administration. Tahir Iqbal: conceptualization, supervision.

## Declarations

**Conflict of interest** The authors declare no competing interests.

## References

- Bermejo M, Aparicio A, Andrés P, López-Sobaler AM, Ortega RM (2007) The influence of fruit and vegetable intake on the nutritional status and plasma homocysteine levels of institutionalised elderly people. *Public Health Nutr*. <https://doi.org/10.1017/S1368980007246580>
- Abiad MG, Meho LI (2018) Food loss and food waste research in the Arab world: a systematic review. *Food Secur*. <https://doi.org/10.1007/s12571-018-0782-7>
- Sandhya (2010) Modified atmosphere packaging of fresh produce: current status and future needs. *LWT - Food Sci. Technol*. <https://doi.org/10.1016/j.lwt.2009.05.018>
- Ijaz M, Zafar M, Afsheen S, Iqbal T (2020) A review on Ag-nanostructures for enhancement in shelf time of fruits. *J Inorg Organomet Polym Mater*. <https://doi.org/10.1007/s10904-020-01504-x>
- Ziani K, Fernández-Pan I, Royo M, & Maté JI (2009). Antifungal activity of films and solutions based on chitosan against typical

- seed fungi. *Food Hydrocoll.* <https://doi.org/10.1016/j.foodhyd.2009.06.005>
6. Ruffo Roberto S, Youssef K, Hashim AF, Ippolito A (2019) Nanomaterials as alternative control means against postharvest diseases in fruit crops. *Nanomaterials.* <https://doi.org/10.3390/nano9121752>
  7. Sardabi F, Mohtadinia J, Shavakhi F, Jafari AA (2014) The effects of 1-methylcyclopropen (1-MCP) and potassium permanganate coated zeolite nanoparticles on shelf life extension and quality loss of golden delicious apples. *J Food Process Preserv.* <https://doi.org/10.1111/jfpp.12197>
  8. Fakruddin M, Hossain Z, Afroz H (2012) Prospects and applications of nanobiotechnology: a medical perspective. *J Nanobiotechnology.* <https://doi.org/10.1186/1477-3155-10-31>
  9. Chaudhary A, Kumar N, Kumar R, Salar RK (2019) Antimicrobial activity of zinc oxide nanoparticles synthesized from Aloe vera peel extract. *SN Appl Sci.* <https://doi.org/10.1007/s42452-018-0144-2>
  10. Naseer M, Aslam U, Khalid B, Chen B (2020) Green route to synthesize zinc oxide nanoparticles using leaf extracts of Cassia fistula and Melia azadarach and their antibacterial potential. *Sci Rep.* <https://doi.org/10.1038/s41598-020-65949-3>
  11. Cai Y, Lim HR, Khoo KS, Ng HS, Cai Y, Wang J, Chan ATY, Show PL (2021) An integration study of microalgae bioactive retention: from microalgae biomass to microalgae bioactives nanoparticle. *Food Chem Toxicol.* <https://doi.org/10.1016/j.fct.2021.112607>
  12. Alghuthaymi MA, Ali AA, Hashim AF, Abd-Elsalam KA (2016) A rapid method for the detection of Ralstonia solanacearum by isolation DNA from infested potato tubers based on magnetic nanotools. *Philipp Agric Sci.* <https://doi.org/10.15436/2377-1372.16.744>
  13. Sharma S, Jaiswal S, Duffy B, Jaiswal AK (2019) Nanostructured materials for food applications: spectroscopy, microscopy and physical properties. *Bioengineering.* <https://doi.org/10.3390/bioengineering6010026>
  14. Vigneshwaran N, Ashtaputre NM, Varadarajan PV, Nachane RP, Paralikal KM, Balasubramanya RH (2007) Biological synthesis of silver nanoparticles using the fungus *Aspergillus flavus*. *Mater Lett.* <https://doi.org/10.1016/j.matlet.2006.07.042>
  15. Ahmad M, Asif S, Klemeš JJ, Mubashir M, Bokhari A, Sultana S, Mukhtar A, Zafar M, Bazmi AA, Khan US, MS, (2022) Conversion of the toxic and hazardous *Zanthoxylum armatum* seed oil into methyl ester using green and recyclable silver oxide nanoparticles. *Fuel.* <https://doi.org/10.1016/j.fuel.2021.122296>
  16. Göl F, Aygün A, Seyrankaya A, Gür T, Yenikaya C, Şen F (2020) Green synthesis and characterization of *Camellia sinensis* mediated silver nanoparticles for antibacterial ceramic applications. *Mater Chem Phys.* <https://doi.org/10.1016/j.matchemphys.2020.123037>
  17. Gulbagca F, Aygün A, Gülcan M, Ozdemir S, Gonca S, Şen F (2021) Green synthesis of palladium nanoparticles: preparation, characterization, and investigation of antioxidant, antimicrobial, anticancer, and DNA cleavage activities. *Appl Organomet Chem.* <https://doi.org/10.1002/aoc.6272>
  18. Meydan I, Seckin H, Burhan H, Gür T, Tanhaei B, Sen F (2022) *Arum italicum* mediated silver nanoparticles: synthesis and investigation of some biochemical parameters. *Environ Res.* <https://doi.org/10.1016/j.envres.2021.112347>
  19. Taqvi SIH, Solangi AR, Buledi JA, Khand NH, Junejo B, Memon AF, Ameen S, Bhatti A, Show PL, Vasseghian Y, Karimi-Maleh H, (2022) Plant extract-based green fabrication of nickel ferrite (NiFe<sub>2</sub>O<sub>4</sub>) nanoparticles: an operative platform for non-enzymatic determination of pentachlorophenol. *Chemosphere.* <https://doi.org/10.1016/j.chemosphere.2022.133760>
  20. Zafar M, Ijaz M, Iqbal T (2021) Efficient Au nanostructures for NIR-responsive controlled drug delivery systems. *Chem Pap.* <https://doi.org/10.1007/s11696-020-01465-y>
  21. Mubashir M, Dumée LF, Fong YY, Jusoh N, Lukose J, Chai WS, Show PL (2021) Cellulose acetate-based membranes by interfacial engineering and integration of ZIF-62 glass nanoparticles for CO<sub>2</sub> separation. *J Hazard Mater.* <https://doi.org/10.1016/j.jhazmat.2021.125639>
  22. Aihara N, Torigoe K, Esumi K (1998) Preparation and characterization of gold and silver nanoparticles in layered laponite suspensions. *Langmuir.* <https://doi.org/10.1021/la980370p>
  23. Lin XZ, Teng X, Yang H (2003) Direct synthesis of narrowly dispersed silver nanoparticles using a single-source precursor. *Langmuir.* <https://doi.org/10.1021/la035185c>
  24. Ijaz M, Zafar M, Islam A, Afsheen S, Iqbal T (2020) A review on antibacterial properties of biologically synthesized zinc oxide nanostructures. *J Inorg Organomet Polym Mater.* <https://doi.org/10.1007/s10904-020-01603-9>
  25. Ijaz M, Zafar M, Iqbal T (2020) Green synthesis of silver nanoparticles by using various extracts: a review. *Inorg Nano-Met Chem.* <https://doi.org/10.1080/24701556.2020.1808680>
  26. Ijaz M, Zafar M (2021) Titanium dioxide nanostructures as efficient photocatalyst: progress, challenges and perspective. *Int J Energy Res.* <https://doi.org/10.1002/er.6079>
  27. Galdiero S, Falanga A, Vitiello M, Cantisani M, Marra V, Galdiero M (2011) Silver nanoparticles as potential antiviral agents. *Molecules.* <https://doi.org/10.3390/molecules16108894>
  28. Meydan I, Burhan H, Gür T, Seçkin H, Tanhaei B, Sen F (2022) Characterization of *Rheum ribes* with ZnO nanoparticle and its antidiabetic, antibacterial, DNA damage prevention and lipid peroxidation prevention activity of in vitro. *Environ Res.* <https://doi.org/10.1016/j.envres.2021.112363>
  29. Seckin H, Tiri RNE, Meydan I, Aygun A, Gunduz MK, Sen F (2022) An environmental approach for the photodegradation of toxic pollutants from wastewater using Pt–Pd nanoparticles: antioxidant, antibacterial and lipid peroxidation inhibition applications. *Environ Res.* <https://doi.org/10.1016/j.envres.2022.112708>
  30. Iqbal T, Raza A, Zafar M, Afsheen S, Kebaili I, Alrobei H (2022) Plant-mediated green synthesis of zinc oxide nanoparticles for novel application to enhance the shelf life of tomatoes. *Appl Nanosci.* <https://doi.org/10.1007/s13204-021-02238-z>
  31. Rambabu K, Bharath G, Banat F, Show PL (2021) Green synthesis of zinc oxide nanoparticles using *Phoenix dactylifera* waste as bioreductant for effective dye degradation and antibacterial performance in wastewater treatment. *J Hazard Mater.* <https://doi.org/10.1016/j.jhazmat.2020.123560>
  32. de Azeredo HM (2013) Antimicrobial nanostructures in food packaging. *Trends Food Sci Technol.* <https://doi.org/10.1016/j.tifs.2012.11.006>
  33. Premanathan M, Karthikeyan K, Jeyasubramanian K, Manivannan G (2011) Selective toxicity of ZnO nanoparticles toward Gram-positive bacteria and cancer cells by apoptosis through lipid peroxidation. *Nanomed.: Nanotechnol. Biol. Med.* <https://doi.org/10.1016/j.nano.2010.10.001>
  34. Iqbal T, Azhar S, Zafar M, Kiran H, Kebaili I, Alrobei H (2021) Synthesis and characterization of Ag-ZnO nano-composites for investigation of variations in the germination of peanut and kidney beans. *Appl Nanosci.* <https://doi.org/10.1007/s13204-021-02244-1>
  35. Bajpai VK, Kamle M, Shukla S, Mahato DK, Chandra P, Hwang SK, Kumar P, Han HuhYS, YK, (2018) Prospects of using nanotechnology for food preservation, safety, and security. *J Food Drug Anal.* <https://doi.org/10.1016/j.jfda.2018.06.011>
  36. Shankar SS, Rai A, Ahmad A, Sastry M (2004) Rapid synthesis of Au, Ag, and bimetallic Au core–Ag shell nanoparticles using

- Neem (*Azadirachta indica*) leaf broth. *J Colloid Interface Sci.* <https://doi.org/10.1016/j.jcis.2004.03.003>
37. Elumalai K., & Velmurugan, S. (2015) Green synthesis, characterization and antimicrobial activities of zinc oxide nanoparticles from the leaf extract of *Azadirachta indica* (L.). *Appl Surf Sci.* <https://doi.org/10.1016/j.apsusc.2015.03.176>
  38. Patra JK, Baek KH (2014) Green nanobiotechnology: factors affecting synthesis and characterization techniques. *J Nanomater.* <https://doi.org/10.1155/2014/417305>
  39. Venu Gopal VR, Kamila S (2017) Effect of temperature on the morphology of ZnO nanoparticles: a comparative study. *Appl Nanosci.* <https://doi.org/10.1007/s13204-017-0553-3>
  40. Rai A, Singh A, Ahmad A, Sastry M (2006) Role of halide ions and temperature on the morphology of biologically synthesized gold nanotriangles. *Langmuir.* <https://doi.org/10.1021/la052055q>
  41. Pandey BD (2012) Synthesis of zinc-based nanomaterials: a biological perspective. *IET Nanobiotechnol.* <https://doi.org/10.1049/iet-nbt.2011.0051>
  42. Amendola V, Bakr OM, Stellacci F (2010) A study of the surface plasmon resonance of silver nanoparticles by the discrete dipole approximation method: effect of shape, size, structure, and assembly. *Plasmonics.* <https://doi.org/10.1007/s11468-009-9120-4>
  43. Roy P, Das B, Mohanty A, Mohapatra S (2017) Green synthesis of silver nanoparticles using *Azadirachta indica* leaf extract and its antimicrobial study. *Appl Nanosci.* <https://doi.org/10.1007/s13204-017-0621-8>
  44. Ahmed S, Saifullah Ahmad M, Swami BL, Ikram S (2016) Green synthesis of silver nanoparticles using *Azadirachta indica* aqueous leaf extract. *J Radiat Res Appl Sci.* <https://doi.org/10.1016/j.matlet.2016.04.126>
  45. He R, Qian X, Yin J, Zhu Z (2002) Preparation of polychrome silver nanoparticles in different solvents. *J Mater Chem.* <https://doi.org/10.1039/B205214H>
  46. Noorjahan CM, Shahina SJ, Deepika T, Rafiq S (2015) Green synthesis and characterization of zinc oxide nanoparticles from Neem (*Azadirachta indica*). *Int J Sci Eng Technol Res.* <https://doi.org/10.1063/5.0002093>
  47. Fakhari S, Jamzad M, Kabiri Fard H (2019) Green synthesis of zinc oxide nanoparticles: a comparison. *Green Chem Lett Rev.* <https://doi.org/10.1080/17518253.2018.1547925>
  48. Jiang Z, Yuan W, Pan H (2005) Luminescence effect of silver nanoparticle in water phase. *Spectrochim Acta - A: Mol Biomol Spectrosc.* <https://doi.org/10.1016/j.saa.2004.09.014>
  49. Anandalakshmi K, Venugobal J, Ramasamy V (2016) Characterization of silver nanoparticles by green synthesis method using *Petalium murex* leaf extract and their antibacterial activity. *Appl Nanosci.* <https://doi.org/10.1007/s13204-015-0449-z>
  50. Ghamsari MS, Alamdari S, Razzaghi D, Pirlar MA (2019) ZnO nanocrystals with narrow-band blue emission. *J Lumin.* <https://doi.org/10.1016/j.jlumin.2018.09.064>
  51. Vafae M, Ghamsari MS (2007) Preparation and characterization of ZnO nanoparticles by a novel sol–gel route. *Mater Lett.* <https://doi.org/10.1016/j.matlet.2006.11.089>
  52. Alamdari S, Sasani Ghamsari M, Lee C, Han W, Park HH, Tafreshi MJ, Afarideh H, Ara MHM (2020) Preparation and characterization of zinc oxide nanoparticles using leaf extract of *Sambucus ebulus*. *Appl Sci.* <https://doi.org/10.3390/app10103620>
  53. Niraimathi KL, Sudha V, Lavanya R, Brindha P (2013) Biosynthesis of silver nanoparticles using *Alternanthera sessilis* (Linn.) extract and their antimicrobial, antioxidant activities. *Colloids Surf B.* <https://doi.org/10.1016/j.colsurfb.2012.08.041>
  54. Jyoti K, Baunthiyal M, Singh A (2016) Characterization of silver nanoparticles synthesized using *Urtica dioica* Linn. leaves and their synergistic effects with antibiotics. *J Radiat Res Appl.* <https://doi.org/10.1016/j.jrras.2015.10.002>
  55. Parashar UK, Kumar V, Bera T, Saxena PS, Nath G, Srivastava SK, Giri R, Srivastava A (2011) Study of mechanism of enhanced antibacterial activity by green synthesis of silver nanoparticles. *Nanotechnology.* <https://doi.org/10.1088/0957-4484/22/41/415104>
  56. Jain S, Mehata MS (2017) Medicinal plant leaf extract and pure flavonoid mediated green synthesis of silver nanoparticles and their enhanced antibacterial property. *Sci Rep.* <https://doi.org/10.1038/s41598-017-15724-8>
  57. Sondi I, Salopek-Sondi B (2004) Silver nanoparticles as antimicrobial agent: a case study on *E. coli* as a model for Gram-negative bacteria. *J. Colloid Interface Sci.* <https://doi.org/10.1016/j.jcis.2004.02.012>
  58. Duran N, Seabra AB (2018) Biogenic synthesized Ag/Au nanoparticles: production, characterization, and applications. *Curr Nanosci.* <https://doi.org/10.2174/1573413714666171207160637>
  59. Wright JB, Lam K, Hansen D, Burrell RE (1999) Efficacy of topical silver against fungal burn wound pathogens. *Am J Infect Control.* [https://doi.org/10.1016/S0196-6553\(99\)70055-6](https://doi.org/10.1016/S0196-6553(99)70055-6)
  60. Eby DM, Schaeublin NM, Farrington KE, Hussain SM, Johnson GR (2009) Lysozyme catalyzes the formation of antimicrobial silver nanoparticles. *ACS Nano.* <https://doi.org/10.1021/nn90079e>
  61. Ankanna STNVKVP, Prasad TNVKV, Elumalai EK, Savithramma N (2010) Production of biogenic silver nanoparticles using *Boswellia ovalifoliolata* stem bark. *Dig J Nanomater Biostruct.* <https://doi.org/10.1007/s10811-012-9851-z>
  62. Sirelkhatim A, Mahmud S, Seeni A, Kaus NHM, Ann LC, Bak-hori SKM, Hasan H, Mohamad D (2015) Review on zinc oxide nanoparticles: antibacterial activity and toxicity mechanism. *Micro Nano Lett.* <https://doi.org/10.1007/s40820-015-0040-x>
  63. Sadeghi B, Gholamhoseinpoor F (2015) A study on the stability and green synthesis of silver nanoparticles using *Ziziphora tenuior* (Zt) extract at room temperature. *Spectrochim Acta A Mol Biomol Spectrosc.* <https://doi.org/10.1016/j.saa.2014.06.046>
  64. Rai M, Yadav A, Gade A (2009) Silver nanoparticles as a new generation of antimicrobials. *Biotechnol Adv.* <https://doi.org/10.1016/j.biotechadv.2008.09.002>
  65. Geethalakshmi R, Sarada DVL (2010) Synthesis of plant-mediated silver nanoparticles using *Trianthema decandra* extract and evaluation of their anti microbial activities. *Int J Eng Sci Technol.* <https://doi.org/10.1016/j.jare.2015.02.007>
  66. Gao L, Li Q, Zhao Y, Wang H, Liu Y, Sun Y, Wang F, Jia W, Hou X (2017) Silver nanoparticles biologically synthesized using tea leaf extracts and their use for extension of fruit shelf life. *IET Nanobiotechnol.* <https://doi.org/10.1049/iet-nbt.2016.0207>
  67. Mohammed Fayaz A, Balaji K, Girilal M, Kalaichelvan PT, Venkatesan R (2009) Mycobased synthesis of silver nanoparticles and their incorporation into sodium alginate films for vegetable and fruit preservation. *J Agric Food Chem.* <https://doi.org/10.1021/jf900337h>
  68. Gudadhe JA, Yadav A, Gade A, Marcato PD, Durán N, Rai M (2014) Preparation of an agar-silver nanoparticles (A-AgNp) film for increasing the shelf-life of fruits. *IET nanobiotechnol.* <https://doi.org/10.1016/j.fpsl.2019.100379>
  69. Emamifar A, Mohammadzadeh M (2015) Preparation and application of LDPE/ZnO nanocomposites for extending shelf life of fresh strawberries. *Food Technol. Biotechnol.* <https://doi.org/10.17113/ftb.53.04.15.3817>
  70. Costa CONTE, Conte A, Buonocore GG, Del Nobile MA (2011) Antimicrobial silver-montmorillonite nanoparticles to prolong the shelf life of fresh fruit salad. *Int J Food Microbiol.* <https://doi.org/10.1016/j.ijfoodmicro.2011.05.018>
  71. Forato LA, de Britto D, de Rizzo JS, Gastaldi TA, Assis OB (2015) Effect of cashew gum-carboxymethylcellulose edible

- coatings in extending the shelf-life of fresh and cut guavas. *Food Packag. Shelf Life*. <https://doi.org/10.1016/j.fpsl.2015.06.001>
72. Haile A, Safawo T (2018) Shelf life and quality of tomato (*Lycopersicon esculentum* Mill.) fruits as affected by different packaging materials. *Afr. J. Food Sci*. <https://doi.org/10.5897/AJFS2017.1568>
73. Abdelmalek GAM, Salaheldin TA (2016) Silver nanoparticles as a potent fungicide for citrus phytopathogenic fungi. *J. Nanomed. Res*. <https://doi.org/10.15406/jnmr.2016.03.00065>
74. He L, Liu Y, Mustapha A, Lin M (2011) Antifungal activity of zinc oxide nanoparticles against *Botrytis cinerea* and *Penicillium expansum*. *Microbiol Res*. <https://doi.org/10.1016/j.micres.2010.03.003>

**Publisher's note** Springer Nature remains neutral with regard to jurisdictional claims in published maps and institutional affiliations.